Coagulation kinetics and aggregate morphology in the intermediate regimes between diffusion-limited and reaction-limited cluster aggregation

D. Asnaghi, M. Carpineti, M. Giglio, and M. Sozzi
Physics Department, University of Milan, via Celoria 16, Milano, Italy
(Received 19 June 1991)

We investigate the kinetics and fractal morphology of aggregating polystyrene latex in an intermediate region between diffusion-limited cluster aggregation (DLCA) and reaction-limited cluster aggregation (RLCA). The measurements are made by means of a low-angle elastic-light-scattering setup covering two decades in scattering wave vectors. For each aggregation run, the salt concentration c is changed and the samples are prepared under isopycnic conditions, to avoid differential sedimentation. The average cluster mass is found to grow according to a power law with an exponent z varying in a continuous fashion in the range of salt concentration used. At high c (DLCA), we find for the fractal morphology $d_f = 1.65$. For lower concentrations, d_f is at first larger than 2 and therefore close to the typical RLCA fractal dimension, but then it gradually reverts to lower values not far from those typical of DLCA. This behavior is also exhibited at the lowest values of c explored, although the decay to DLCA is much slower. An interpretation of the results is presented on the basis of the available theories and simulation work on the cluster morphology in the intermediate regimes.

PACS number(s): 64.60.Cn, 05.40.+j, 82.70.Dd

INTRODUCTION

Over the last decade a large amount of work has been produced in the area of colloidal aggregation, both theoretically [1–6] and experimentally [7–16]. There are various reasons for this upsurge of interest in the field. Among them is the fact that both theory and experiments have shown that universality features are exhibited when the aggregation process occurs according to two well-defined regimes [13–15], those of diffusion-limited cluster aggregation (DLCA) and reaction-limited cluster aggregation (RLCA). In these regimes the sticking probability between monomers is assumed to be equal to one or much smaller than one, respectively. Experimentally the sticking probability is varied by adding to a solution of stable colloids some reagents that screen or reduce at will the Coulombic stabilizing interaction.

The two most prominent features associated with the universal behavior are the reaction kinetics and the cluster morphology. The theory predicts that the average cluster mass should grow linearly in time for DLCA and exponentially for RLCA, the fractal dimensions of the clusters being close to 1.8 and 2.1, respectively.

Most of the experimental work has been done in these two regimes, and there is striking evidence that if the reacting solutions are properly arranged to meet the DLCA or RLCA conditions, then universality features are indeed observed, irrespective of the details of the systems under investigation.

The work on pure DLCA and RLCA has been so influential as to often generate the incorrect impression that all the aggregation processes should fall into either one of these two modes.

In this work we have investigated by means of static low-angle light scattering the kinetics and cluster morphology of polystyrene colloids aggregating under conditions between DLCA and RLCA. We will call these regimes "intermediate."

The description of the reaction kinetics is usually given in terms of the Smoluchowski equation [17]. Unfortunately, analytical solutions are known only for a few simple forms of the kernels appearing in the equation. To overcome this difficulty and in order to describe the intermediate regimes, dynamic-scaling concepts have been introduced [18] by parametrization of the kernels in terms of only two scaling coefficients. Asymptotic expressions for the cluster distributions and for the evolution average quantities are thus derived at the expense of a minimal budget of *ad hoc* assumptions.

Alternatively, simulation work [19,20] and preliminary experimental observations [21] suggest that the intermediate regimes could be described as a crossover between RLCA and DLCA, although no analytical work to describe such a transition has been produced so far.

Additional and complementary characterization of colloidal aggregation comes from the analysis of the aggregate morphology. In this regard, we have studied whether the aggregates still retain dilation symmetry in the intermediate regimes and, if so, how the fractal dimension changes as one moves from DLCA towards RLCA. Indeed, although simulation work has been produced on this topic and provides interesting predictions [19], supporting experimental evidence is still lacking.

THEORY

We will briefly recall some of the results of the dynamic-scaling solutions of the Smoluchowski equation [17]

 © 1992 The American Physical Society

$$\frac{dc_n}{dt}=\frac{1}{2}\sum_{\substack{i,j\\ i+j=n}} k(i,j)c_i c_j - c_n \sum_{i=1}^{\infty} k(n,i)c_i \ , \qquad n=1,\ldots,\infty \quad (1)$$

where c_n describes the concentration of clusters made up with n monomers. It is a rather crude description of the system since it is valid in the mean-field limit. Most of the nonsimulation theoretical predictions are, however, based on this equation, where all the physics is contained in the expressions of the kernels $k(ij)$. It is commonly assumed [18] that they are homogeneous functions of the arguments i and j,

$$k(ai,aj)\sim a^{\lambda}k(i,j) \ , \quad \lambda \leq 2 \ , \quad (2)$$

$$k(i,j)\sim i^{\mu}j^{\nu} \quad (j \gg i) \ , \quad \nu \leq 1 \quad (3)$$

where the restrictions on λ and ν arise from the interpenetrability of clusters.

The previous relations provide a classification of the kernels by means of the two exponents λ and μ ($\nu=\lambda-\mu$). Let us recall here their physical meaning.

Since a is supposed to be a large positive constant, the homogeneity parameter λ describes the reactivity of two big clusters. It accounts for the tendency of the system to form large aggregates in a short time. Moreover this parameter is strongly related to the aggregation kinetic, since, as indicated above, $\lambda=0$ corresponds to DLCA while $\lambda=1$ yields RLCA. Values larger than 1 imply gelation, namely, the formation of an infinite cluster at a finite time. Scaling arguments have been used [18] to predict that in the intermediate regimes the growth of the average mass is given by

$$M=t^{1/(1-\lambda)} \ , \quad 0<\lambda<1 \ . \quad (4)$$

Values of λ at variance with those characteristic of DLCA and RLCA have been reported in a recent paper [22] but very little work has been done to investigate in a systematic way the intermediate regimes.

The exponent μ describes whether big-cluster–big-cluster or big-cluster–small-cluster aggregations are favored, and therefore is a control parameter for the cluster-size distribution. No restriction is imposed on this exponent, and its sign is the all-important element. In fact, for $\mu<0$ the aggregation between a big cluster and a small one is favored and the cluster distribution is monodisperse. On the contrary, for $\mu>0$ the interaction between two big clusters is stronger and the system is polydisperse. When $\mu=0$ neither the former kind of reaction nor the latter plays a special role. The prediction is, however, that the distribution is still polydisperse to some extent.

THE EXPERIMENTAL SETUP

Since the fractal morphology can be best evaluated from the asymptotic behavior of the scattered intensity, we have used a low-angle scattering setup covering almost two decades in scattering wave vectors, from $q=4\times10^2$ to $q=3\times10^4$ cm^{-1}.

It has already been described in previous papers [12,23], so we will recall here simply that the measurements are taken at 30 scattering wave vectors equally spaced on a log plot. Light scattered from the sample is collected by a lens and focused on a multielement monolithic sensor. Each element is shaped in the form of a quarter of an annulus centered around a tiny hole through which the transmitted beam is allowed to pass clear of the sensors. Two additional sensors are used. One is placed behind the transmitted beam pinhole to monitor transmitted beam power. The other collects a small portion of the incoming beam power via a low reflectivity beam splitter placed before the scattering cell. Since the system collects light at small angles, there is no possibility to avoid stray-light contributions. Consequently, prior to each run a blank measurement is taken with the scattering cell filled with the solvent alone. These blank measurements are then used to correct the scattering data by properly taking into account both incoming beam intensity variations and the sample turbidity. The sample thickness is selected so as to give a scattering signal large enough to make stray-light corrections reasonably small.

The sample is made of surfactant-free polystryrene spheres 0.13 μm in diameter suspended in a mixture of water and heavy water so as to make the solvent density as close as possible to the density of the polystyrene spheres. Divalent salt ($MgCl_2$) is used to promote the aggregation. We found that a 30 mM concentration is adequate to generate pure DLCA. The salt content is then lowered to cover the intermediate region toward RLCA, while the polystyrene concentration is kept equal to 5×10^{10} monomers/cm^3.

EXPERIMENTAL RESULTS

In order to extract estimates of the average cluster mass M, average radius of gyration R_G, and fractal dimension d_f, we have tried to fit the scattered intensity distributions with the easiest guess possible for the structure factor, namely, with the Fisher-Burford (FB) function [24]:

$$S(q)=\frac{S(0)}{[1+(qR_G)^2/\frac{3}{2}d_f]^{d_f/2}} \ . \quad (5)$$

The choice was prompted by the fact that in previous studies on fast DLCA aggregation we found that it did fit the data quite nicely [12]. We have also assumed that the cluster-size distribution is monodisperse. This assumption is consistent with the fact that $\mu<0$ corresponds to DLCA and $\mu=0$ to RLCA [25], so a reasonable guess for the intermediate regimes is $\mu<0$. We show in Fig. 1 a fit to scattering intensity data taken at an intermediate value of the salt concentration, where (as we will show later) the reaction kinetics was definitely at variance with the DLCA behavior. In the fitting procedure [26] the $I(q=0)$ value, the average radius of gyration, and the fractal dimension were kept floating. As one can notice, the fit is very good, and we have not attempted to utilize different expressions other than FB since we estimated that the quality of the fit could hardly be improved.

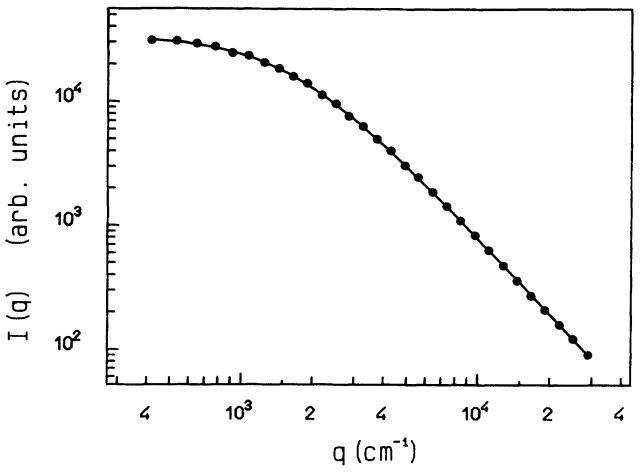

FIG. 1. Typical nonlinear least-squares fit of experimental data in the intermediate regimes ($[MgCl_2]=14$ mM) with the Fisher-Burford function.

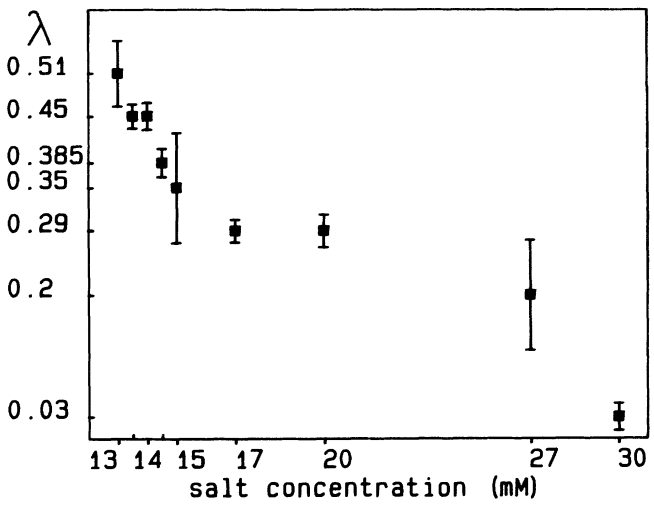

FIG. 3. Behavior of the homogeneity coefficient λ as a function of salt concentration.

Furthermore, since the average mass comes from the $I(q=0)$ extrapolated value [6], it is reasonable that such an estimate would not be strongly dependent on the choice of the fitting function.

In Fig. 2 we plot the dependence of the average mass on aggregation time t. The data are shown for two limiting concentrations, namely, $c=13.5$ mM and $c=30$ mM. In both cases the data can be fitted with a power-law growth and it is quite evident that the exponent z becomes larger as the salt concentration is diminished. Cases at intermediate values of the salt concentration c are not shown to avoid overcrowding, but power-law growth is always observed. If these data are interpreted on the basis of dynamic-scaling solutions, then $z=1/(1-\lambda)$ and one can extract the dependence of λ on salt concentration c. The data are shown in Fig. 3. One can notice that the variation is fairly smooth and λ changes from $\lambda=0.03$ to $\lambda=0.51$. Of course if dynamic scaling is inapplicable, then the interpretation of the data in terms of λ is meaningless. Comments about this point are included in the last section.

We point out that we could not study the kinetics at lower values of salt concentration because the duration of the runs becomes unacceptably long. Indeed the time required to collect the data at the lowest concentration is already two days. Incidentally, we have also performed runs under nonisopycnic conditions, using water instead of the water–heavy-water mixture as a solvent. Under these conditions, reaction rates are definitely faster (by a factor between 2 and 3). We attribute this speeding up to sedimentation effects. It is worth mentioning that while at low salt concentration the dependence of M on t re-

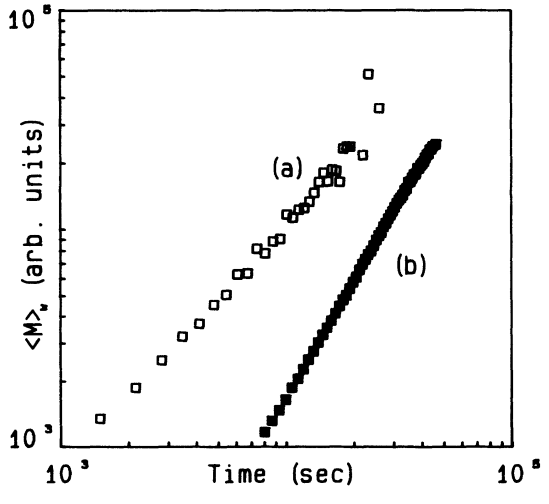

FIG. 2. Log-log plot of $\langle M\rangle_W$ vs t for two limiting salt concentrations: (a) $c=30$ mM, (b) $c=13.5$ mM. Since $\langle M\rangle_W \propto t^z = t^{1/(1-\lambda)}$, the slope gives an estimate of z and consequently of λ.

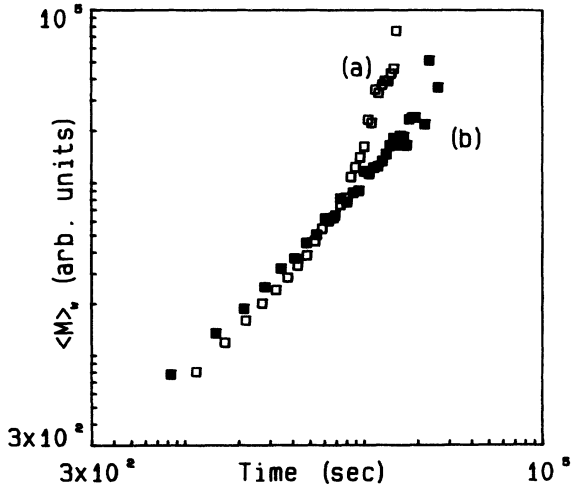

FIG. 4. Log-log plot of $\langle M\rangle_W$ vs t for a nonisopycnic run (a) and an isopycnic run (b). Both curves are for $c=30$ mM (DLCA).

tains the same power-law behavior, at high salt concentration (close to DLCA) there is a marked difference between isopycnic and nonisopycnic conditions (Fig. 4). Although in the early phases both water and water–heavy-water solutions give $M \propto t$, later on nonisopycnic samples exhibit a quite evident and repeatable accelerated growth.

At present we have no explanation why reactions closer to DLCA show larger deviations between isopycnic and nonisopycnic conditions when compared to what happens for reactions closer to RLCA. Simulation work in this area would be very useful to clarify this issue.

We now present the results concerning the fractal morphology of the clusters grown in the intermediate regimes. As we indicated in the experimental section, we derive from each plot of the scattered intensity as a function of the scattered wave vector an estimate of the fractal dimension d_f, so we are able to recover the time evolution of d_f for each aggregation run in the intermediate cases. The data are shown in Fig. 5, and refer to three runs. Curve (a) refers to one of the largest salt concentrations ($c = 27$ mM), (b) to an intermediate case ($c = 17$ mM), while (c) corresponds to one of the lowest concentrations ($c = 14$ mM). Curve (a) is close to a pure DLCA growth. Correspondingly the value of d_f is rather low, $d_f = 1.68$, and in agreement with the findings of a previous study [12]. It is worth noticing that the value of d_f does not change during the entire run, the data being scattered around a stable value. The behavior of curve (b), at variance, starts from a larger value, close to 2, and then decays to a value close to that of curve (a). Finally, curve (c) stays close to $d_f = 2.03$, a value typical of RLCA, in the initial stages of the aggregation and then exhibits a slow decay.

The following comments are appropriate. First, it is quite surprising that such a large value for d_f is actually observed before the reaction kinetics attains the exponential growth typical of the RLCA regime. Accordingly, fractal morphology has a quicker response than the kinetics to changes in the sticking probability. Second, and most interesting [curve (b)], the dimension changes during the course of the reaction, starting from values not far from the RLCA value, and then reverting to a level close to that typical of DLCA. This is in contrast with the definition of a fractal as a scale invariant, self-similar object. Its structure is described by a unique fractal dimension irrespective of the actual size of the cluster. This is the case of DLCA and RLCA and is in agreement with the results presented here for case (a) shown in Fig. 5.

To understand what happens in the regimes far from both DLCA and RLCA, notice that by choosing the FB function for the fitting procedure we tacitly assume that the clusters are ideal fractals. Strictly speaking, we therefore derive an "effective" fractal dimension. Its strong dependence on time, i.e., on the aggregate size, means that the way clusters meet and stick to one another changes during the growth. Indeed it has been pointed out [20] that at the beginning monomers can freely wander among the branches of the growing clusters, due to the low sticking probability and this results in a dense packing. As the clusters grow, however, the number of points of contact increases too and the effective sticking probability is higher. So the clusters do not succeed in interpenetrating each other as they used to do when they were small. According to this picture one should not be surprised to observe more tenuous structures and lower fractal dimensions as the reaction proceeds.

To further corroborate the data above, and again ignoring that the clusters in the intermediate regimes are not fractals in a strict sense, we have plotted for each run the average mass as a function of the radius. For true fractals, a log-log plot would give a slope equal to d_f, since $M \propto R_G^{d_f}$. A plot of this type is shown in Fig. 6. One can see that the data fall initially on a straight line. The value of d_f thus derived is in good agreement with the value determined at the early stages via the fitting of $I(q)$ with the FB function. Later one, however, the data

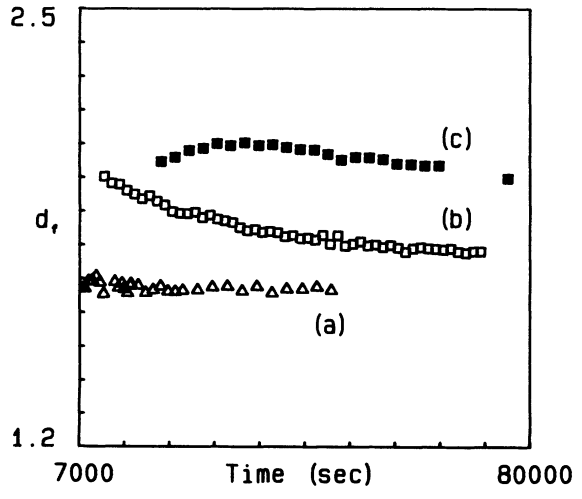

FIG. 5. Behavior of the fractal dimension as a function of time for three salt concentrations: (a) $c = 27$ mM, (b) $c = 17$ mM, (c) $c = 14$ mM.

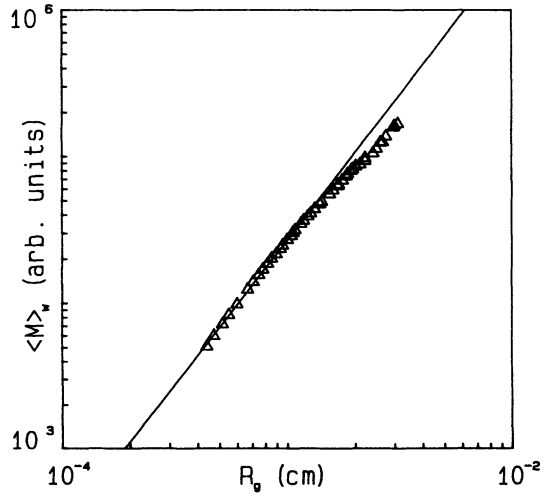

FIG. 6. Log-log plot of $\langle M \rangle_w$ vs R_G for $c = 13$ mM (intermediate regimes).

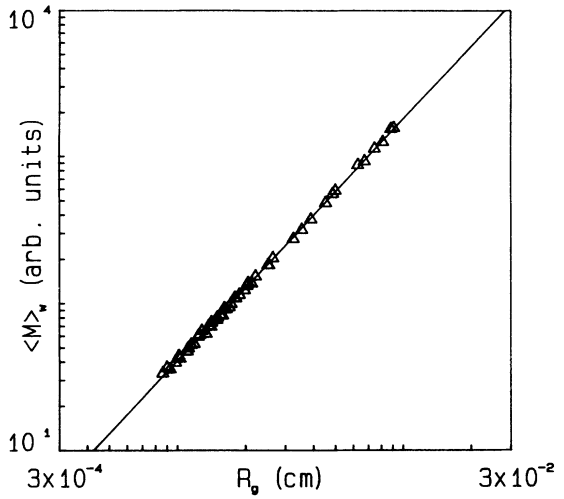

FIG. 7. Log-log plot of $\langle M \rangle_W$ vs R_G for a DLCA ($c = 30$ mM). The slope gives an estimate of d_f.

tend to align on a smaller slope, thus confirming that the fractal dimension decreases. On the contrary, Fig. 7 shows that in the case of DLCA no sign of change of slope is noticeable in the plot of M versus R_G.

These experimental results can be interpreted on the basis of a simulation work by Kolb and Jullien [19] in connection with the morphology in the intermediate regimes. The authors do predict that for sticking probability between 1 and 0, a crossover should exist. Consequently they suggest a generalized fractality reaction

$$M \propto R_G^{d_f} f\left[\frac{R_G}{\xi_0}\right] \tag{6}$$

where ξ_0 is a characteristic interpenetration length depending on the sticking probability and independent of R_G, and $f(R_G/\xi_0)$ is an unspecified function.

To illustrate it, they show log-log plots of $R(p=1)/R(p)$ as a function of the mass of the cluster. For $p=1$ the ratio is of course equal to one and describes the DLCA mode. As p is decreased, the plots start with a finite slope, but show a rolloff, and the slope eventually decreases and tends to align itself to a horizontal asymptote. The position of the rolloff shifts to larger values of the cluster mass as p is reduced. For $p=0$ a straight line with the appropriate slope is also reported, indicating the pure RLCA mode.

The experimental results shown in Fig. 5 are therefore in qualitative agreement with the findings of Kolb and Jullien. A quantitative comparison is not possible at this stage.

CONCLUSIONS

Working with isopycnic and unsheared samples we have investigated by means of static light scattering the kinetics of aggregation under conditions that are intermediate between DLCA and RLCA.

The data show that the rate of growth of the weight average cluster mass follows a power law. If these data are compared with the dynamic-scaling solutions for the Smoluchowski equation [18], the only available analytical solution so far, good agreement is found, and the so-called homogeneity exponent λ varies in a range quite consistent with the scaling hypothesis ($0 \leq \lambda \leq 1$). Within this scenario one could then conclude that regimes at variance with DLCA and RLCA do exist and no crossover between the two is actually taking place. An alternative explanation, however, could be presented on the basis of the morphology results.

They show that although under DLCA conditions rather typical d_f values are found, for intermediate values of the electrolyte the "effective" fractal dimension changes during the course of the reaction, first attaining larger values, typical of RLCA, and then reverting to values not far from those typical of DLCA. Consequently the morphology data strongly suggest that,, as the average cluster mass grows, diffusion becomes the prevailing limiting process and the aggregation crosses over to a diffusion-limited one [21].

In order to reconcile such a behavior with the reported time evolution of the average cluster mass, one has then to assume that the plots shown in Fig. 2 cannot be considered as truly asymptotic. This would suggest that, if measurements could be performed at later times, a crossover in the kinetics should eventually become evident. This alternative picture is quite interesting and stimulating, but further work, both theoretical and experimental, is highly desirable.

ACKNOWLEDGMENTS

Helpful conversations with R. Jullien are kindly acknowledged. We also wish to thank D. A. Weitz for having suggested the interpretation of the data in terms of a crossover behavior. Finally we thank E. Paganini and U. Perini for help with the instrumentation.

This work has been supported by grants from the Ministero dell' Università e della Ricerca Scientifica e Tecnologica (MURST) and the Consiglio Nazionale delle Ricerche (CNR).

[1] See, for example, *Kinetics of Aggregation and Gelation,* edited by F. Family and D. P. Landau (North-Holland, Amsterdam, 1984).

[2] T. A. Witten, Jr. and L. M. Sander, Phys. Rev. Lett. **47**, 1400 (1981)

[3] P. Meakin, Phys. Rev. Lett. **51**, 1119 (1983).

[4] W. D. Brown and R. C. Ball, J. Phys. A **18**, L517 (1985).

[5] P. G. J. van Dongen and M. H. Ernst, in *Fractals in Physics,* edited by L. Pietronero and E. Tosatti (North-Holland, Amsterdam, 1986), p. 303.

[6] J. E. Martin and B. J. Ackerson, Phys. Rev. A **31**, 1180 (1985).

[7] M. Matsushita, K. Sumida, and Y. Sawada, J. Phys. Soc. Jpn. **54**, 2786 (1985).

[8] C. Aubert and D. S. Cannell, Phys. Rev. Lett. **56**, 738 (1986).
[9] J. E. Martin, Phys. Rev. A **36**, 3415 (1987).
[10] G. Bolle, C. Cametti, P. Codastefano, and P. Tartaglia, Phys. Rev. A **35**, 837 (1987).
[11] J. P. Wilcoxon, J. E. Martin, and D. Schaefer, Phys. Rev. A **39**, 2675 (1989).
[12] M. Carpineti, F. Ferri, M. Giglio, E. Paganini, and U. Perini, Phys. Rev. A **42**, 7347 (1990).
[13] M. Y. Lin, H. M. Lindsay, D. A. Weitz, R. C. Ball, R. Klein, and P. Meakin, J. Phys. Condens. Matter **2**, 3093 (1990).
[14] M. Y. Lin, H. M. Lindsay, D. A. Weitz, R. C. Ball, R. Klein, and P. Meakin, Phys. Rev. A **41**, 2005 (1990).
[15] M. Y. Lin, H. M. Lindsay, D. A. Weitz, R. C. Ball, R. Klein, and P. Meakin, Proc. R. Soc. London, Ser. A **423**, 71 (1989).
[16] M. Y. Lin, R. Klein, H. M. Lindsay, D. A. Weitz, R. C. Ball, and P. Meakin, J. Colloid Interface Sci. **137**, 263 (1990).
[17] M. von Smoluchowski, Phys. Z **17**, 593 (1916).
[18] P. G. J. van Dongen and M. H. Ernst, Phys. Rev. Lett. **54**, 1396 (1985).
[19] M. Kolb and R. Jullien, J. Phys. (Paris) Lett. **45**, L977 (1984).
[20] F. Family, P. Meakin, and T. Vicsek, J. Chem. Phys. **83**, 4144 (1985).
[21] D. A. Weitz, J. S. Huang, M. Y. Lin, and J. Sung, Phys. Rev. Lett. **54**, 1416 (1985).
[22] B. J. Olivier and C. M. Sorensen, Phys. Rev. A **41**, 2093 (1990).
[23] F. Ferri, M. Giglio, E. Paganini, and U. Perini, Europhys. Lett. **7**, 599 (1988).
[24] M. E. Fisher and R. J. Burford, Phys. Rev. A **156**, 583 (1967).
[25] J. E. Martin, J. P. Wilcoxon, D. Schaefer, and J. Odinek, Phys. Rev. A **41**, 4379 (1990).
[26] MINUIT (FORTRAN, 2891 cards); F. James and M. Ross, Comput. Phys. Commun. **10**, 343 (1975).